Science

RESEARCH ARTICLE

Cite as: M. Isinger *et al.*, *Science* 10.1126/science.aao7043 (2017).

Photoionization in the time and frequency domain

M. Isinger,[1]* R.J. Squibb,[2] D. Busto,[1] S. Zhong,[1] A. Harth,[1] D. Kroon,[1] S. Nandi,[1] C. L. Arnold,[1] M. Miranda,[1] J. M. Dahlström,[1,3] E. Lindroth,[3] R. Feifel,[2] M. Gisselbrecht,[1] A. L'Huillier[1]

[1]Department of Physics, Lund University, P.O. Box 118, SE-22 100 Lund, Sweden. [2]Department of Physics, Gothenburg University, Origovägen 6B, SE-41 296 Göteborg, Sweden. [3]Department of Physics, Stockholm University, SE-106 91 Stockholm, Sweden.

*Corresponding author. Email: marcus.isinger@fysik.lth.se

Ultrafast processes in matter, such as the electron emission following light absorption, can now be studied using ultrashort light pulses of attosecond duration (10^{-18} s) in the extreme ultraviolet spectral range. The lack of spectral resolution due to the use of short light pulses has raised issues in the interpretation of the experimental results and the comparison with theoretical calculations. We determine photoionization time delays in neon atoms over a 40 eV energy range with an interferometric technique combining high temporal and spectral resolution. We spectrally disentangle direct ionization from ionization with shake-up, in which a second electron is left in an excited state, and obtain excellent agreement with theoretical calculations, thereby solving a puzzle raised by 7-year-old measurements.

While femtosecond lasers allow for the study and control of the motion of nuclei in molecules, attosecond light pulses give access to even faster dynamics, such as electron motion induced by light-matter interactions (*1*). During the last decade, seminal experiments with sub-femtosecond temporal resolution have allowed the observation of the electron valence motion (*2*), monitoring of the birth of an autoionizing resonance (*3*, *4*) or the decay of a core vacancy (*5*). Fast electron motion occurs even when electrons are directly emitted from materials upon absorption of sufficiently energetic radiation (the photoelectric effect). The time for the photoelectron emission (*6*), called photoionization time delay (*7*, *8*), is typically of the order of tens of attoseconds, depending on the excitation energy and on the underlying ionic core structure.

Photoemission has traditionally been studied in the frequency domain, using high-resolution photoelectron spectroscopy with x-ray synchrotron radiation sources, and such methods have provided a detailed understanding of the electronic structure of matter (*9*, *10*). Absorption of light in the 60-100 eV range by Ne atoms, for example, leads to direct ionization in the 2s or 2p shells and to processes mediated by electron-electron interaction, leaving the residual ion in an excited state (often called shake-up) or doubly ionized (*11*–*13*).

It may be argued that the high temporal resolution achieved in attosecond experiments prevents any spectral accuracy and thus may affect the interpretation of experimental results. This is especially true when different processes can be induced simultaneously and lead to photoelectrons with kinetic energies within the bandwidth of the excitation pulse. In fact, the natural trade-off between temporal and spectral resolution may be circumvented, as beautifully shown in the visible spectrum using high-resolution frequency combs based upon phase-stable femtosecond pulse trains (*14*).

Here, we bridge the gap between high-resolution photoelectron spectroscopy and attosecond dynamics, making use of the high-order harmonic spectrum obtained by phase-stable interferences between attosecond pulses in a train. Photoionization time delays of the 2s and 2p shells are measured in neon over a broad energy range from 65 to 100 eV, with high temporal (20 as) and spectral (200 meV) accuracy. Our spectral resolution comes from the sharpness of the harmonic comb teeth (harmonic bandwidth). Time delays are obtained by measuring spectral phase derivatives with an interferometric technique originally introduced for characterizing attosecond pulses in a train, called RABITT (Reconstruction of Attosecond Beating by Interference of Two-photon Transition) (*15*, *16*). Temporal accuracy requires a stable and reproducible broadband extreme ultraviolet (XUV) waveform. In the limit of long infrared (IR) pulses, the temporal resolution is only limited by the stability of the interferometer and the spectral resolution by the resolving power of the electron spectrometer.

Our spectral resolution allows us to disentangle direct 2s ionization from shake-up processes, in which a 2p electron is ionized while a second is excited to a 3p state (*11*, *17*, *18*). The experimental results for the difference between 2s and 2p time delays (Fig. 1A, yellow and red dots) agree with theoretical calculations performed within the framework of many-body perturbation theory (the solid black line). Our experimental observation of a shake-up process (diamonds) due to electron correlation also provides a possible explanation for the discrepancy between the pioneering result of Schultze *et al.* (*7*) (square) and theoretical calculations (*19*–*21*).

Photoionization time delays

In general, measured time delays can be considered as the

sum of two contributions, $\tau_{XUV} + \tau_A$, where the first term is the group delay of the broadband excitation XUV field and the second term reflects the influence of the atomic system (*15*). To eliminate the influence of the excitation pulse, two measurements can be performed simultaneously, for example, on different ionization processes (*7*, *8*, *22–24*) or in different target species (*25–28*). This enables the determination of relative photoionization time delays. Absolute photoionization delays can be deduced if we assume that one of the delays can by sufficiently accurately calculated to serve as an absolute reference (*24*).

In non-resonant conditions, the atomic delay can in turn be approximated as the sum of two contributing delays, $\tau_A \approx \tau_W + \tau_{cc}$. The first term is the group delay of the electronic wave packet created by absorption of XUV radiation, also called photoionization time delay or Wigner delay. Wigner interpreted the derivative of the scattering phase as the group delay of the outgoing electronic wave-packet in a collision process (*29*). The second term, τ_{cc}, is a substantial correction to the atomic time delay due to the interaction of the laser probe field with the Coulomb potential. At high kinetic energies τ_{cc} can be accurately calculated using either the asymptotic form of the wave function (*30*) or by classical trajectories (*31*) which makes it possible to extract τ_W given τ_A. The subscript "cc" refers to the fact that the delay arises from stimulated IR transitions between two continuum states (*30*). It is now understood that this delay is identical to the so-called Coulomb-laser coupling delay, τ_{CLC}, used in the context of attosecond streaking (*31*). When multiple angular channels may have comparable amplitude (*26*) as is the case close to resonances (*25*, *27*, *32*) or for low kinetic energy electrons (*23*), the separation of the two contributions τ_W and τ_{cc} may become ambiguous.

Experimental method

Femtosecond laser pulses from a Titanium-Sapphire laser system fed a Mach-Zehnder-like interferometer [for a complete experimental description, see (*33*)]. In one arm, high harmonics were generated from neon atoms. Two sets of metallic foils were used to filter the XUV spectra: a combination of zirconium and aluminum foils, yielding a narrow bandpass filter letting through three harmonics (yellow spectrum in Fig. 1B) and a set of two zirconium foils, filtering harmonics above 70 eV (red spectrum in Fig. 1B). In the second arm of the interferometer, the intensity and delay of an IR probe pulse could be adjusted. Both pulses were recombined and focused by a toroidal mirror into a magnetic bottle electron spectrometer, with high collection efficiency and good spectral resolution (≤100 meV).

Interferometric technique

Figure 2 illustrates the principle of our interferometric measurement when using the Al-Zr filter combination. Two-photon ionization leads to sidebands which can be reached by two pathways: absorption of one harmonic and an IR photon, and by absorption of the next harmonic together with emission of one IR photon (Fig. 2A) (*15*). Ionization of one subshell by the high-order harmonics and the IR field results in five electron peaks: three peaks due to single-photon ionization by harmonics 41, 43 and 45 and two peaks due to sidebands 42 and 44. Since for this filter set the XUV spectrum spans less than 15 eV and the difference in the ionization energies of the Ne 2s and 2p subshells is 26.8 eV (*11*, *12*), the spectra generated from the two subshells are energetically well separated (Fig. 2B). Figure 2C shows the variation of the spectrum as a function of the delay τ between the XUV and IR fields. The intensity of the sidebands oscillates according to (*8*)

$$S(\tau) = \alpha + \beta \cos[2\omega(\tau - \tau_{XUV} - \tau_A)] \qquad (1)$$

where α and β are delay-independent and ω denotes the IR frequency (π/ω = 1.3 fs in our experiment). Our analysis consists in determining the phase and amplitude of the signal oscillating at 2ω by fitting Eq. 1 to the experimental data. The delay τ_{XUV} depends only on the excitation pulse, which is the same for the 2s and 2p ionization paths. The difference in the photoionization time delays can therefore be obtained by comparing the oscillations of the sidebands corresponding to the same absorbed energy (e.g., S42), involving the same harmonics (H41 and H43). We note that the time delay differences that can be measured in this type of experiments should not exceed the period of the oscillations, equal to half the laser cycle, 1.3 fs. Our analysis is performed over the bandwidth of the excitation pulse, from 60 to 75 eV in the experiment with the Al-Zr filters (yellow spectrum in Fig. 1B) and from 80 to 100 eV using the Zr-filters (red spectrum).

Shake-up

If the different energy components of the sideband are in phase, the analysis can be performed on the energy-integrated signal. Following the method described in (*3*), we analyze the sideband oscillations across its spectrum, in steps of 50 meV. Figure 3 illustrates how this method allows us to identify shake-up processes and eliminate their influence on the 2s-time delay measurement. In Fig. 3A, we indicate two competing ionization pathways leading to overlapping electron spectra: 2s-ionization by absorption of H57 and emission of one IR photon (S56); 2p-ionization and excitation $2p \rightarrow 3p$ by absorption of H61. Similarly, 2s-ionization by absorption of H57 and two-photon shake-up (H61+IR) overlap. Although

a number of shake-up processes come into play at photon energies above 50 eV, shake-up to the $2p^4(^1D)3p(^2P^0)$ state, with binding energy equal to 55.8 eV, is the most intense (*12*, *20*), reaching one sixth of the amplitude of 2s-ionization and is thus comparable to a 2s-sideband. A comparison between the photoelectron spectra with and without IR shown in Fig. 3B shows the effect of shake-up on the right side of the 2s-sideband. In Fig. 3C, the amplitude and phase of the 2ω oscillation, obtained by Fourier transforming the signal, is shown as a function of energy. The phase is strongly modified in the region of overlap between $H61_{su}$ and $S56_{2s}$. In general, harmonic and sideband oscillate out of phase, so that, with poor spectral resolution, even a weak shake-up harmonic signal strongly influences the phase of a partially overlapping 2s-ionization sideband signal. The spectrally-resolved phase of the 2p-sidebands (not shown) is completely flat, owing to the fact that this region is free from resonances or shake-up states (*20*). The time delays indicated in Fig. 1A have been obtained by selecting a flat spectral region for the 2s-phase determination, avoiding shake-up processes. We could also estimate the difference in time delay between shake-up and 2p-ionization, by analyzing the shake-up sidebands amplitude and phase (see $S62_{su}$ on the right side in Fig. 3C). The results are shown as diamonds in Fig. 1A. The error bars are generally quite high, due to low signal-to-noise ratio.

Comparison of theory and experiment

The key results obtained in the present work are summarized in Fig. 1A. For the experimental results (yellow and red dots, corresponding to the spectra shown in B), the indicated error bars correspond to the standard deviation from ten spectrograms, weighted with the quality of the fitted sideband oscillations. The difference in time delay is negative, which indicates that 2p-ionization is slightly delayed compared to 2s-ionization, and decreases as the excitation energy increases. Unfortunately, we could not determine delays at energies higher than 100 eV due to overlap between electrons created by 2s-ionization with 100 eV photon energy and those by 2p-ionization with 70 eV. The difference in ionization energy between the two subshells corresponds almost exactly to 17ω, rendering the electrons indistinguishable with our current spectral resolution.

Figure 1A also presents calculations using a many-body perturbation theory approach for the treatment of electron correlation effects (*21*). Here, we calculate τ_A by using lowest-order perturbation theory for the radiation fields. The interaction with the XUV photon is assumed to initiate the photoionization process. The laser photon then acts perturbatively on the photoelectron to drive a transition to an uncorrelated final state, computed by solving an approximate Schrödinger equation with a static spherical potential of the final ion. Using this method with ab-initio Hartree-Fock orbitals, it has been shown that the atomic delay from the 2p state in neon is insensitive to inter-orbital correlation, while the coupling of the 2s orbital is advanced by a few attoseconds due to coupling to the 2p orbital (*21*). Here the calculations are improved further by using the experimental binding energies for both 2p and 2s and the calculations are performed for averaged emission over all angles to mimic the experimental conditions. The theoretical results are indicated by the solid black line in Fig. 1A. We emphasize that the excellent agreement obtained between theory and experiment for the difference in time delays between 2s and 2p ionization requires the careful energy-resolved analysis of the experimental data presented above and the disentanglement between 2s-ionization and shake-up.

Absolute photoionization time delays

Figure 4 presents more details about the calculations and illustrates the different contributions to the measured time delay differences. In Fig. 4A, the black curve represents the Wigner delay $\tau_W(2p)$, calculated for an emission angle in the direction of the light polarization, while the dashed curve is the angle-averaged time delay, defined as $\tau_1(2p) = \tau_A(2p) - \tau_{cc}(2p)$. The difference between the two curves is at most two attoseconds, which demonstrates a small angle-dependence of the 2p time delay. Indeed, in this energy region, ionization toward the s continuum is much lower than toward the d continuum, which may justify the approximation of $\tau_1(2p)$ as the Wigner delay for the d-channel, but not on the level of a few attoseconds. Figure 4B shows the same quantities for 2s-ionization. Here, the difference between $\tau_1(2s)$ and $\tau_W(2s)$ is not visible, which justifies the interpretation of $\tau_1(2s)$ as Wigner delay. The colored dots and square have been obtained by subtracting from the experimental data (see Fig. 1A) the calculated $\tau_A(2p)$ for the angle-integrated case and the continuum-continuum contribution $\tau_{cc}(2s)$, thus extracting the absolute Wigner delays for 2s-ionization for the first time. The 2s Wigner time delay does not vary with energy in this region and is approximately equal to –3 attoseconds. Other calculations of the 2s Wigner delays (*20*, *34*) agree well with our experimental result. We stress that the increase with excitation energy observed in Fig. 1A reflects essentially the energy dependence of $\tau_{cc}(2s) - \tau_{cc}(2p)$, which itself is dominated by the variation of $\tau_{cc}(2s)$.

Solving a 7-year-old puzzle

We compared our theoretical results with calculations in the conditions of an attosecond streak-camera experiment, i.e., with a stronger IR field, a single attosecond pulse and angle-resolved detection (*20*), obtaining agreement for the Wigner delays, the τ_{cc} and time delay differences within a few attoseconds. Then, we carried out an energy-integrated instead of

energy-resolved analysis of the sideband oscillations and obtained time delay differences which were, in general, below those indicated in Fig. 1A, close to the value retrieved in (*7*). This leads us to suggest that the discrepancy of the experimental result (*7*) with theory (*19*–*21*) might be due to the influence of shake-up processes, not resolved and accounted for in the analysis of the experiment (*35*).

The good agreement obtained between our experimental data and numerical calculations of the photoionization time delays from the 2s and 2p shells in neon for photon energies ranging from 65 eV up to 100 eV gives us confidence in this type of measurement for other, more complex, atomic or molecular systems, and point out the necessity for keeping high frequency resolution in addition to high temporal resolution. Our method can be improved by using longer laser pulses, allowing for the generation of trains with reproducible attosecond pulses (high temporal resolution) and narrow harmonic bandwidth (high spectral resolution), in combination with highly stable optical interferometer and an electron spectrometer with high resolving power. The use of lasers in the mid-IR region for harmonic generation (*36*) will have several other advantages: broader XUV spectra (*37*), better energy sampling and access to time scales of a few femtoseconds of great interest for photochemistry applications. Our approach provides the means to study and control photo-induced processes both in the time and frequency domain from the visible to the x-ray range.

REFERENCES AND NOTES

1. F. Krausz, M. Ivanov, Attosecond physics. *Rev. Mod. Phys.* **81**, 163–234 (2009). doi:10.1103/RevModPhys.81.163
2. E. Goulielmakis, Z.-H. Loh, A. Wirth, R. Santra, N. Rohringer, V. S. Yakovlev, S. Zherebtsov, T. Pfeifer, A. M. Azzeer, M. F. Kling, S. R. Leone, F. Krausz, Real-time observation of valence electron motion. *Nature* **466**, 739–743 (2010). doi:10.1038/nature09212 Medline
3. V. Gruson, L. Barreau, Á. Jiménez-Galan, F. Risoud, J. Caillat, A. Maquet, B. Carré, F. Lepetit, J.-F. Hergott, T. Ruchon, L. Argenti, R. Taïeb, F. Martín, P. Salières, Attosecond dynamics through a Fano resonance: Monitoring the birth of a photoelectron. *Science* **354**, 734–738 (2016). doi:10.1126/science.aah5188 Medline
4. A. Kaldun, A. Blättermann, V. Stooß, S. Donsa, H. Wei, R. Pazourek, S. Nagele, C. Ott, C. D. Lin, J. Burgdörfer, T. Pfeifer, Observing the ultrafast buildup of a Fano resonance in the time domain. *Science* **354**, 738–741 (2016). doi:10.1126/science.aah6972 Medline
5. M. Drescher, M. Hentschel, R. Kienberger, M. Uiberacker, V. Yakovlev, A. Scrinzi, T. Westerwalbesloh, U. Kleineberg, U. Heinzmann, F. Krausz, Time-resolved atomic inner-shell spectroscopy. *Nature* **419**, 803–807 (2002). doi:10.1038/nature01143 Medline
6. A. L. Cavalieri, N. Müller, T. Uphues, V. S. Yakovlev, A. Baltuška, B. Horvath, B. Schmidt, L. Blümel, R. Holzwarth, S. Hendel, M. Drescher, U. Kleineberg, P. M. Echenique, R. Kienberger, F. Krausz, U. Heinzmann, Attosecond spectroscopy in condensed matter. *Nature* **449**, 1029–1032 (2007). doi:10.1038/nature06229 Medline
7. M. Schultze, M. Fiess, N. Karpowicz, J. Gagnon, M. Korbman, M. Hofstetter, S. Neppl, A. L. Cavalieri, Y. Komninos, T. Mercouris, C. A. Nicolaides, R. Pazourek, S. Nagele, J. Feist, J. Burgdörfer, A. M. Azzeer, R. Ernstorfer, R. Kienberger, U. Kleineberg, E. Goulielmakis, F. Krausz, V. S. Yakovlev, Delay in photoemission. *Science* **328**, 1658–1662 (2010). doi:10.1126/science.1189401 Medline
8. K. Klünder, J. M. Dahlström, M. Gisselbrecht, T. Fordell, M. Swoboda, D. Guénot, P. Johnsson, J. Caillat, J. Mauritsson, A. Maquet, R. Taïeb, A. L'Huillier, Probing single-photon ionization on the attosecond time scale. *Phys. Rev. Lett.* **106**, 143002 (2011). doi:10.1103/PhysRevLett.106.143002 Medline
9. V. Schmidt, Photoionization of atoms using synchrotron radiation. *Rep. Prog. Phys.* **55**, 1483–1659 (1992). doi:10.1088/0034-4885/55/9/003
10. U. Becker, D. A. Shirley, *VUV and Soft X-Ray Photoionization* (Springer Science and Business Media, 2012).
11. S. Svensson, B. Eriksson, N. Martensson, G. Wendin, U. Gelius, Electron shake-up and correlation satellites and continuum shake-off distributions in x-ray photoelectron spectra of the rare gas atoms. *J. Electron Spectrosc. Relat. Phenom.* **47**, 327–384 (1988). doi:10.1016/0368-2048(88)85020-5
12. U. Becker, R. Wehlitz, O. Hemmers, B. Langer, A. Menzel, Observation of participator Auger decay following valence photoionization with excitation. *Phys. Rev. Lett.* **63**, 1054–1057 (1989). doi:10.1103/PhysRevLett.63.1054 Medline
13. P. Lablanquie, F. Penent, R. I. Hall, J. H. D. Eland, P. Bolognesi, D. Cooper, G. C. King, L. Avaldi, R. Camilloni, S. Stranges, M. Coreno, K. C. Prince, A. Müehleisen, M. Z˘itnik, Observation and characterization of the fluorescence decay of the $2s2p^6\ np^1\ P^0$ excited states of Ne. *Phys. Rev. Lett.* **84**, 431–434 (2000). doi:10.1103/PhysRevLett.84.431 Medline
14. A. Marian, M. C. Stowe, J. R. Lawall, D. Felinto, J. Ye, United time-frequency spectroscopy for dynamics and global structure. *Science* **306**, 2063–2068 (2004). doi:10.1126/science.1105660 Medline
15. P. M. Paul, E. S. Toma, P. Breger, G. Mullot, F. Auge, P. Balcou, H. G. Muller, P. Agostini, Observation of a train of attosecond pulses from high harmonic generation. *Science* **292**, 1689–1692 (2001). doi:10.1126/science.1059413 Medline
16. Y. Mairesse, A. de Bohan, L. J. Frasinski, H. Merdji, L. C. Dinu, P. Monchicourt, P. Breger, M. Kovacev, R. Taïeb, B. Carré, H. G. Muller, P. Agostini, P. Salières, Attosecond synchronization of high-harmonic soft x-rays. *Science* **302**, 1540–1543 (2003). doi:10.1126/science.1090277 Medline
17. A. Kikas, S. J. Osborne, A. Ausmees, S. Svensson, O. P. Sairanen, S. Aksela, High-resolution study of the correlation satellites in photoelectron spectra of the rare gases. *J. Electron Spectrosc. Relat. Phenom.* **77**, 241–266 (1996). doi:10.1016/0368-2048(95)02552-9
18. P. Bolognesi, L. Avaldi, D. R. Cooper, M. Coreno, R. Camilloni, G. C. King, High-resolution threshold photoelectron measurements of the $Ne^+\ 2p^4n\ell$ satellite states. *J. Phys. B* **35**, 2927–2948 (2002). doi:10.1088/0953-4075/35/13/307
19. L. R. Moore, M. A. Lysaght, J. S. Parker, H. W. van der Hart, K. T. Taylor, Time delay between photoemission from the 2p and 2s subshells of neon. *Phys. Rev. A* **84**, 061404 (2011). doi:10.1103/PhysRevA.84.061404
20. J. Feist, O. Zatsarinny, S. Nagele, R. Pazourek, J. Burgdörfer, X. Guan, K. Bartschat, B. I. Schneider, Time delays for attosecond streaking in photoionization of neon. *Phys. Rev. A* **89**, 033417 (2014). doi:10.1103/PhysRevA.89.033417
21. J. M. Dahlström, T. Carette, E. Lindroth, Diagrammatic approach to attosecond delays in photoionization. *Phys. Rev. A* **86**, 061402 (2012). doi:10.1103/PhysRevA.86.061402
22. E. P. Månsson, D. Guénot, C. L. Arnold, D. Kroon, S. Kasper, J. M. Dahlström, E. Lindroth, A. S. Kheifets, A. L'Huillier, S. L. Sorensen, M. Gisselbrecht, Double ionization probed on the attosecond timescale. *Nat. Phys.* **10**, 207–211 (2014). doi:10.1038/nphys2880
23. S. Heuser, Á. Jiménez Galán, C. Cirelli, C. Marante, M. Sabbar, R. Boge, M. Lucchini, L. Gallmann, I. Ivanov, A. S. Kheifets, J. M. Dahlström, E. Lindroth, L. Argenti, F. Martín, U. Keller, Angular dependence of photoemission time delay in helium. *Phys. Rev. A* **94**, 063409 (2016). doi:10.1103/PhysRevA.94.063409
24. M. Ossiander, F. Siegrist, V. Shirvanyan, R. Pazourek, A. Sommer, T. Latka, A. Guggenmos, S. Nagele, J. Feist, J. Burgdörfer, R. Kienberger, M. Schultze, Attosecond correlation dynamics. *Nature* **13**, 280 (2016). doi:10.1038/nphys3941
25. C. Palatchi, J. M. Dahlström, A. S. Kheifets, I. A. Ivanov, D. M. Canaday, P. Agostini, L. F. DiMauro, Atomic delay in helium, neon, argon and krypton. *J. Phys. B* **47**, 245003 (2014). doi:10.1088/0953-4075/47/24/245003
26. D. Guénot, D. Kroon, E. Balogh, E. W. Larsen, M. Kotur, M. Miranda, T. Fordell, P. Johnsson, J. Mauritsson, M. Gisselbrecht, K. Varjù, C. L. Arnold, T. Carette, A. S. Kheifets, E. Lindroth, A. L′ Huillier, J. M. Dahlström, Measurements of relative photoemission time delays in noble gas atoms. *J. Phys. B* **47**, 245602 (2014).

doi:10.1088/0953-4075/47/24/245602
27. M. Lucchini, L. Castiglioni, L. Kasmi, P. Kliuiev, A. Ludwig, M. Greif, J. Osterwalder, M. Hengsberger, L. Gallmann, U. Keller, Light-matter interaction at surfaces in the spatiotemporal limit of macroscopic models. *Phys. Rev. Lett.* **115**, 137401 (2015). doi:10.1103/PhysRevLett.115.137401 Medline
28. I. Jordan, M. Huppert, S. Pabst, A. S. Kheifets, D. Baykusheva, H. J. Wörner, Spin-orbit delays in photoemission. *Phys. Rev. A* **95**, 013404 (2017). doi:10.1103/PhysRevA.95.013404
29. E. P. Wigner, Lower limit for the energy derivative of the scattering phase shift. *Phys. Rev.* **98**, 145–147 (1955). doi:10.1103/PhysRev.98.145
30. J. M. Dahlström, D. Guénot, K. Klünder, M. Gisselbrecht, J. Mauritsson, A. L'Huillier, A. Maquet, R. Taïeb, Theory of attosecond delays in laser-assisted photoionization. *Chem. Phys.* **414**, 53–64 (2013). doi:10.1016/j.chemphys.2012.01.017
31. S. Nagele, R. Pazourek, J. Feist, K. Doblhoff-Dier, C. Lemell, K. Tőkési, J. Burgdörfer, Time-resolved photoemission by attosecond streaking: Extraction of time information. *J. Phys. B* **44**, 081001 (2011). doi:10.1088/0953-4075/44/8/081001
32. M. Kotur, D. Guénot, Á. Jiménez-Galán, D. Kroon, E. W. Larsen, M. Louisy, S. Bengtsson, M. Miranda, J. Mauritsson, C. L. Arnold, S. E. Canton, M. Gisselbrecht, T. Carette, J. M. Dahlström, E. Lindroth, A. Maquet, L. Argenti, F. Martín, A. L'Huillier, Spectral phase measurement of a Fano resonance using tunable attosecond pulses. *Nat. Commun.* **7**, 10566 (2016). doi:10.1038/ncomms10566 Medline
33. Materials and methods are available as supplementary materials.
34. A. S. Kheifets, Time delay in valence-shell photoionization of noble-gas atoms. *Phys. Rev. A* **87**, 063404 (2013). doi:10.1103/PhysRevA.87.063404
35. We note, however, that the influence of shake-up processes on the streaking experiment of (*7*) is investigated theoretically in (*21*) and not found to explain the difference between theory and experiment.
36. B. Sheehy, J. D. D. Martin, L. F. DiMauro, P. Agostini, K. J. Schafer, M. B. Gaarde, K. C. Kulander, High harmonic generation at long wavelengths. *Phys. Rev. Lett.* **83**, 5270–5273 (1999). doi:10.1103/PhysRevLett.83.5270
37. T. Popmintchev, M.-C. Chen, D. Popmintchev, P. Arpin, S. Brown, S. Alisauskas, G. Andriukaitis, T. Balciunas, O. D. Mücke, A. Pugzlys, A. Baltuska, B. Shim, S. E. Schrauth, A. Gaeta, C. Hernández-García, L. Plaja, A. Becker, A. Jaron-Becker, M. M. Murnane, H. C. Kapteyn, Bright coherent ultrahigh harmonics in the keV x-ray regime from mid-infrared femtosecond lasers. *Science* **336**, 1287–1291 (2012). doi:10.1126/science.1218497 Medline
38. B. L. Henke, E. M. Gullikson, J. C. Davis, X-ray interactions: Photoabsorption, scattering, transmission, and reflection at E = 50-30,000 eV, Z = 1-92. *At. Data Nucl. Data Tables* **54**, 181–342 (1993). doi:10.1006/adnd.1993.1013
39. D. Kroon, D. Guénot, M. Kotur, E. Balogh, E. W. Larsen, C. M. Heyl, M. Miranda, M. Gisselbrecht, J. Mauritsson, P. Johnsson, K. Varjú, A. L'huillier, C. L. Arnold, Attosecond pulse walk-off in high-order harmonic generation. *Opt. Lett.* **39**, 2218–2221 (2014). doi:10.1364/OL.39.002218 Medline
40. J. H. D. Eland, O. Vieuxmaire, T. Kinugawa, P. Lablanquie, R. I. Hall, F. Penent, Complete two-electron spectra in double photoionization: The rare gases Ar, Kr, and Xe. *Phys. Rev. Lett.* **90**, 053003 (2003). doi:10.1103/PhysRevLett.90.053003 Medline

ACKNOWLEDGMENTS

A.L. thanks Jun Ye for fruitful discussions. This research was supported by the European Research Council (Advanced Grant PALP 339253), the Swedish Research Council (Grant No. 2013-8185), and the Knut and Alice Wallenberg Foundation. J.M.D. was funded by the Swedish Research Council, Grant No. 2014-3724. The authors declare that they have no competing interests. All data and analysis details presented in this work are available upon request to M.I.

SUPPLEMENTARY MATERIALS

www.sciencemag.org/cgi/content/full/science.aao7043/DC1
Materials and Methods
References (*39*, *40*)

22 August 2017; accepted 19 October 2017
Published online 2 November 2017
10.1126/science.aao7043

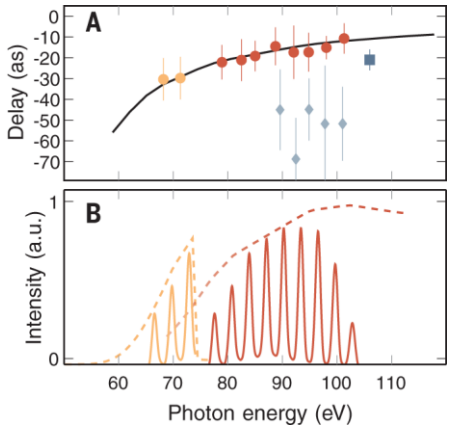

Fig. 1. Photoionization time delays in neon. (**A**) Time delay differences [τ_A(2s) −τ_A(2p)] in neon as a function of photon energy for the two spectra shown in (B) (yellow and red dots). Theoretical calculations within many-body perturbation theory (black solid line) agree very well with the experimental data. Also shown is the streaking experiment from (*7*) (square), as well as the measured time delay differences [τ_A(su) − τ_A(2p)] between shake-up and 2p-ionization (diamonds). (**B**) Photon spectra used in the measurement. High-order harmonics are generated in neon gas and filtered with a combination of 200 nm thick Al and Zr filters (yellow spectrum) and with two Zr filters (red spectrum). The dashed lines illustrate the transmission curves of the two combinations of filters (*38*).

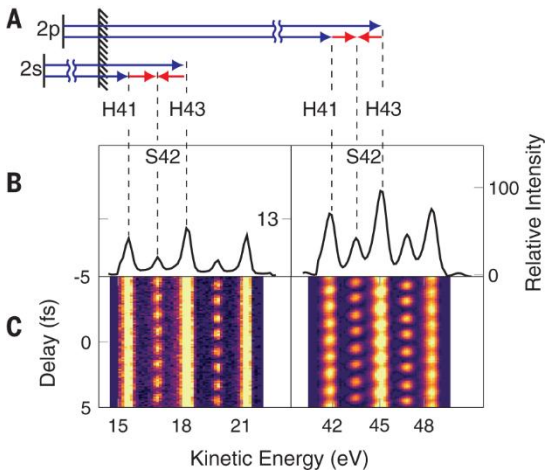

Fig. 2. Principle of the interferometric technique. (A) Kinetic energy diagram for ionization from the 2s and 2p subshells using XUV (blue arrows) and IR (red arrows) radiation. (B) Time-averaged photoelectron spectrum obtained with Al-Zr-filtered harmonics. For both the 2s and 2p subshells, ionization results in three peaks due to absorption of harmonics (H41, H43, and H45) and two sidebands peaks (S42 and S44) reachable via two-color two-photon transitions. (C) Photoelectron spectrum as function of delay between the XUV pulse train and the IR field. The sideband amplitudes strongly oscillate as a function of delay.

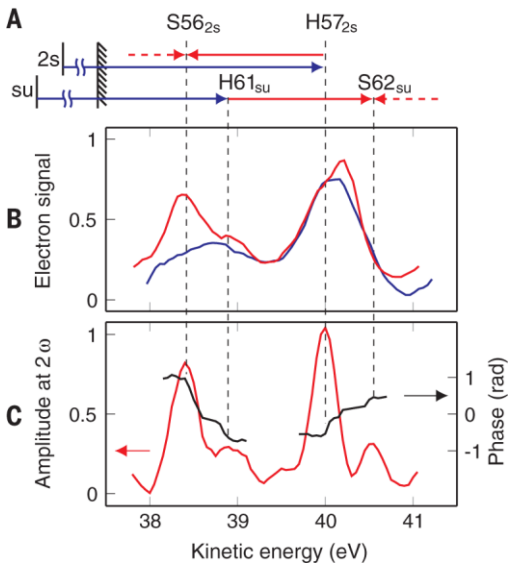

Fig. 3. Energy-resolved interferometric technique and identification of shake-up process. (**A**) Kinetic energy diagram for 2s- and 2p-ionization accompanied by 2p → 3p excitation (shake-up). The difference in threshold energy for these two processes is approximately 7.4 eV (*11*, *17*). (**B**) Photoelectron spectra obtained with XUV only (blue) and XUV + IR (red). The electron peak due to shake-up induced by absorption of H61 partly overlaps with S56 from 2s-ionization. The shoulder on the S56 (red spectrum) can be attributed to one-photon induced shake-up. (**C**) Energy resolved intensity and phase of the 2ω-oscillation, obtained by Fourier transforming the signal. The shake-up harmonic oscillates out of phase with the sideband, causing a sudden drop in the energy-resolved phase. The sideband originating from the shake-up state can be distinguished on the right side, allowing for a separate analysis of its time delay.

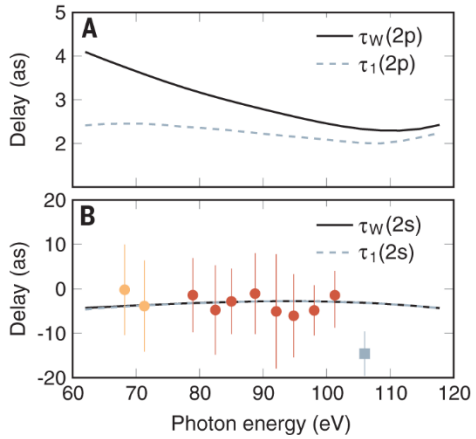

Fig. 4. Absolute photoionization time delays. (A) Calculated Wigner delay $\tau_W(2p)$ along the direction of the light polarization as a function of the photon energy (black solid line). The dashed line indicates the angle-averaged one photon ionization time delay accessible in the experiment. The difference between the two quantities is less than two attoseconds over the whole energy range. (B) Same as in (A) for 2s-ionization. The difference between $\tau_W(2s)$ and $\tau_1(2s)$ is not visible. The experimental data (this work, yellow and red dots and (*7*), square) is transformed to $\tau_1(2s)$ by subtraction of the analytical $\tau_{cc}(2s)$ and simulated $\tau_1(2p)$.

Science

Photoionization in the time and frequency domain

M. Isinger, R.J. Squibb, D. Busto, S. Zhong, A. Harth, D. Kroon, S. Nandi, C. L. Arnold, M. Miranda, J. M. Dahlström, E. Lindroth, R. Feifel, M. Gisselbrecht and A. L'Huillier

published online November 2, 2017